

# Substrate Adhesion of a Nongrafted Flexible Polymer in a Cavity

Michael Bachmann\* and Wolfhard Janke†

*Institut für Theoretische Physik, Universität Leipzig,*

*Augustusplatz 10/11, D-04109 Leipzig, Germany*

## Abstract

In a contact density chain-growth study we investigate the solubility-temperature pseudo-phase diagram of a lattice polymer in a cavity with an attractive surface. In addition to the main phases of adsorbed and desorbed conformations we find numerous subphases of collapsed and expanded structures.

PACS numbers: 05.10.-a, 87.15.Aa, 87.15.Cc

arXiv:0710.4314v1 [cond-mat.soft] 23 Oct 2007

---

\*E-mail: Michael.Bachmann@itp.uni-leipzig.de

†E-mail: Wolfhard.Janke@itp.uni-leipzig.de;

Homepage: <http://www.physik.uni-leipzig.de/CQT.html>

## I. INTRODUCTION

The requirement of higher integration scales in electronic circuits, the onset of nanosensory applications in biomedicine, but also the fascinating capabilities of modern experimental setup with its enormous potential in polymer and surface research recently led to an increasing interest at the hybrid interface of organic and inorganic matter [1, 2, 3, 4, 5]. This also includes numerous detailed studies, e.g., of polymer film wetting phenomena [6, 7], pattern recognition [8, 9], protein–ligand binding and docking [10, 11, 12], charged adsorbed polymers [13] as well as deposition and growth of polymers at surfaces [14].

In most theoretical and computational studies the polymer is anchored at the substrate with one of its ends which reduces the entropic freedom of the polymer. These surface-grafted polymers [15, 16, 17, 18, 19, 20] are, e.g., of particular interest in studies of shape transformations [21], e.g., as reaction to external fields [22, 23, 24]. However, in many recent experiments of organic–inorganic interfaces the setup is different [2, 3] and is more adequately described by a polymer moving in a cavity with one adsorbing surface [25, 26]. The main difference of such nongrafted polymers considered in this work is of entropic kind: In the desorbed phase the polymer can move freely within the cavity, and the polymer can fold into conformations, where the ends have no contact with the surface.

This paper is organized as follows. In Sect. II we describe the details of a minimalistic model for the hybrid system. The main result, the solubility-temperature pseudo-phase diagram, is presented and discussed in Sect. III. The interpretation is consolidated by exemplified studies of fluctuations and correlations of relevant thermodynamic quantities such as numbers of contacts between monomers and monomer-substrate contacts as well as the gyration tensor, in the different phases. The contact numbers turn out to be adequate system parameters for the description of the macrostate of the system, and therefore the free energy in dependence of these contact numbers is subject of a detailed study in Sect. IV. This quantity is also useful for classifying the conformational transitions between the phases which are also discussed there. Eventually, we conclude in Sect. V with a summary of the main results.

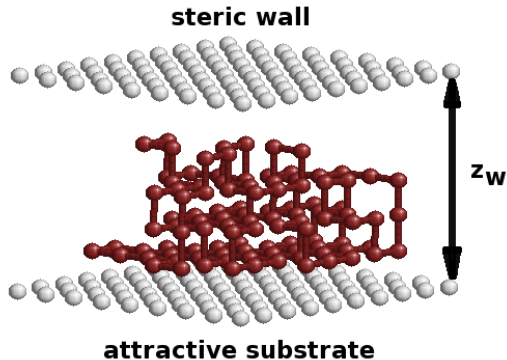


FIG. 1: Cavity model used in this work. The lower of the two parallel surfaces is attractive to the polymer, the upper is steric only. The distance between the surfaces is  $z_w$  lattice units.

## II. MINIMALISTIC MODEL FOR POLYMER ADSORPTION

We employ a minimalistic simple-cubic (sc) lattice model [25] which allows a systematic analysis of the conformational phases experienced by a nongrafted polymer in a cavity with one adhesive surface. An example for the cavity model is shown in Fig. 1. The polymer can move between the two infinitely extended parallel planar walls, separated by a distance  $z_w$  expressed in lattice units. The substrate is short-range attractive to the monomers of the polymer chain, while the influence of the other wall is purely steric.

Denoting the number of nearest-neighbor, but nonadjacent monomer-monomer contacts by  $n_m$  and the number of nearest-neighbor monomer-substrate contacts by  $n_s$ , the energy of the hybrid system can be expressed in the simplest model as

$$E_s(n_s, n_m) = -\varepsilon_s n_s - \varepsilon_m n_m, \quad (1)$$

where  $\varepsilon_s$  and  $\varepsilon_m$  are the respective contact energy scales, which are left open in the following. For simplicity, we perform a simple rescaling and set  $\varepsilon_s = \varepsilon_0$  and  $\varepsilon_m = \varepsilon_0 s$ . Here we have introduced the overall energy scale  $\varepsilon_0$  and the dimensionless reciprocal solubility  $s$  that controls the quality of the implicit solvent surrounding the polymer (the larger the  $s$ , the worse the solvent). Since contacts with the substrate usually entail a reduction of monomer-monomer contacts, there are two competing forces (rated against each other by the energy scales) affecting the formation of intrinsic and surface contacts. In this paper we mainly focus on the conformational transitions the polymer experiences under different environmental conditions. Concretely, we are interested in the dependence of energetic

and structural quantities on temperature  $T$  and reciprocal solubility  $s$  in equilibrium. The probability (per unit area) for a conformation with  $n_s$  surface and  $n_m$  monomer-monomer contacts at temperature  $T$  and reciprocal solubility  $s$  is given by

$$p_{T,s}(n_s, n_m) = \frac{1}{Z} g_{n_s n_m} e^{\varepsilon_0(n_s + s n_m)/k_B T}, \quad (2)$$

where  $g_{n_s n_m} = \delta_{n_s 0} g_{n_m}^u + (1 - \delta_{n_s 0}) g_{n_s n_m}^b$  is the contact density and  $Z$  the partition sum. In this decomposition,  $g_{n_m}^u$  stands for the density of unbound conformations, whereas  $g_{n_s n_m}^b$  is the density of surface and intrinsic contacts of all conformations bound to the substrate. Obviously, the number of the conformations without contact to the attractive substrate,  $g_{n_m}^u$ , depends on the distance  $z_w$  between the cavity walls. For a sufficiently large distance  $z_w$  from the substrate the influence of the neutral surface on the unbound polymer is small. For  $z_w \rightarrow \infty$ , however,  $g_{n_m}^u$  formally diverges. Therefore, the non-adhesive, impenetrable steric wall is necessary for regularization.

We studied polymers with up to 200 monomers by applying the contact-density chain-growth algorithm which is an improved variant of the recently developed multicanonical chain-growth sampling method [27, 28]. All these methods set up on a variant of the pruned-enriched variant [29] of Rosenbluth sampling [30]. The main advantage of the improved method is that it directly samples the contact density  $g_{n_s n_m}$ , which is very useful for problems, where the model provides different energy scales. This generalizes the ordinary multicanonical version [27] which samples the density of states, i.e., the number of states for given energy. Here we can set the two independent energy scales  $\varepsilon_m$  and  $\varepsilon_s$  or their ratio  $s$ , respectively, *after* the simulation. This allows to introduce the reciprocal solubility  $s$  as a second environmental parameter in addition to the temperature  $T$ .

The partition sum of the system as a function of these two parameters is simply  $Z = \sum_{n_s, n_m} g_{n_s n_m} \exp\{\varepsilon_0(n_s + s n_m)/k_B T\}$  and the statistical average of any function  $O(n_s, n_m)$  is given by the formula

$$\langle O \rangle(T, s) = \sum_{n_s, n_m} O(n_s, n_m) p_{T,s}(n_s, n_m), \quad (3)$$

which is very convenient since it only requires to estimate the contact density  $g_{n_s n_m}$  in the simulation. Denoting contact correlation matrix elements as  $M_{xy}(T, s) = \langle xy \rangle_c = \langle xy \rangle -$

$\langle x \rangle \langle y \rangle$  with  $x, y = n_s, n_m$ , the specific heat can be written as

$$C_V(T, s) = k_B \left( \frac{\varepsilon_0}{k_B T} \right)^2 (1, s) M(T, s) \begin{pmatrix} 1 \\ s \end{pmatrix}. \quad (4)$$

All quantities depending only on the contact numbers  $n_m$  and  $n_s$  can therefore simply be calculated from the estimate of the contact density  $g_{n_s n_m}$  provided by our simulation method.

Although the two contact parameters are sufficient to describe the macrostate of the system and their fluctuations characterize the main pseudo-phase transition lines, it is often useful to introduce also nonenergetic quantities such as the end-to-end distance and the gyration tensor for gaining more detailed structural information of the polymer. For our specific problem at hand it is particularly useful to study the structural anisotropy of the adsorbed polymer in the different phases. To this end, we define the general gyration tensor for a polymer chain of  $N$  beads with the components

$$R_{ij}^2 = \frac{1}{N} \sum_{n=1}^N \left( x_i^{(n)} - \bar{x}_i \right) \left( x_j^{(n)} - \bar{x}_j \right), \quad (5)$$

where  $x_i^{(n)}$ ,  $i = 1, 2, 3$ , is the  $i$ th Cartesian coordinate of the  $n$ th monomer and  $\bar{x}_i = \sum_{n=1}^N x_i^{(n)} / N$  is the center of mass with respect to the  $i$ th coordinate. Anisotropy in the polymer fluctuations is connected with the system's geometry and therefore it will be sufficient to study the components of the gyration tensor parallel ( $x, y$  components) and perpendicular (in  $z$  direction) to the planar walls,

$$R_{\parallel}^2 = \frac{1}{N} \sum_{n=1}^N \left[ \left( x^{(n)} - \bar{x} \right)^2 + \left( y^{(n)} - \bar{y} \right)^2 \right] \quad (6)$$

and

$$R_{\perp}^2 = \frac{1}{N} \sum_{n=1}^N \left( z^{(n)} - \bar{z} \right)^2. \quad (7)$$

The gyration radius is then simply the trace of the gyration tensor,  $R_{\text{gyr}}^2 = \text{Tr} R^2 = \sum_{i=1}^3 R_{ii}^2 = R_{\parallel}^2 + R_{\perp}^2$ . The calculation of statistical averages for quantities  $R$  that are not necessarily functions of the contact numbers  $n_s$  and  $n_m$  cannot be performed via Eq. (3). In this case only the more general relation  $\langle R \rangle = \sum_{\mathbf{X}} R(\mathbf{X}) \exp\{-E_s(\mathbf{X})/k_B T\} / Z$  holds, where the sum runs over all polymer conformations  $\mathbf{X}$ . Introducing the accumulated density  $R_{\text{acc}}(n'_s, n'_m) = \sum_{\mathbf{X}} R(\mathbf{X}) \delta_{n_s(\mathbf{X}) n'_s} \delta_{n_m(\mathbf{X}) n'_m} / Z$ , where  $\delta_{ij}$  is the Kronecker symbol, the expectation value can be expressed, however, in a form similar to Eq. (3):

$$\langle R \rangle = \sum_{n_s, n_m} R_{\text{acc}}(n_s, n_m) e^{-E_s(n_s, n_m)/k_B T}. \quad (8)$$

The quantity  $R_{\text{acc}}(n_s, n_m)$  can easily be measured in simulations with the contact density chain-growth algorithm. In the following we use natural units, i.e., we set  $k_B = \varepsilon_0 \equiv 1$ .

### III. THERMODYNAMIC BEHAVIOR OF THE HYBRID SYSTEM

For our exemplified study of the hybrid system in equilibrium we chose a polymer with 179 monomers. Since this is a prime number, the polymer is unable to form perfect cuboid conformations on the sc lattice, as it is, e.g., the case for a 100-mer. [25] There we found two low-temperature subphases dominated by the same  $4 \times 5 \times 5$  cuboid. In one subphase it had 20 surface contacts, while in the other the cuboid was simply rotated, entailing 25 surface contacts. This is a typical example, where the exact number of monomers in the linear chain is directly connected with the occurrence of such specific pseudo-phases which are not, of course, phases in the traditional view. Nonetheless, the enormous progress in high-resolution experimental structure analyses and in the technological equipment for precise polymer deposition, as well as the natural finite length of classes of polymers (e.g., peptides and proteins), explain the growing interest in pseudo-phases and the conformational transitions between them. Here we mainly focus on the expected thermodynamic phase transitions [16, 17] and low-temperature higher-order layering pseudo-phase transitions [19]. The following results were obtained from contact-density chain-growth simulations of the 179-mer in a cavity with  $z_w = 200$  (see Fig. 1), choosing uniformly distributed starting points at random. In eight independent runs  $1.6 \times 10^9$  polymer conformations were generated in total. The resulting contact density  $g_{n_s n_m}$  and accumulated densities like  $R_{\text{acc}}(n_s, n_m)$  are independent of external parameters such as temperature  $T$  and reciprocal solubility  $s$ . Concrete values of statistical quantities for specific parameter settings are obtained by simple reweighting as in Eqs. (2) and (8).

#### A. Solubility-temperature pseudo-phase diagram

Discontinuities or divergences of energetic and nonenergetic fluctuations as functions of external parameters reveal typically dramatic cooperative transitions in the collective, macroscopic behavior of the system's microscopic degrees of freedom in the thermodynamic limit. These transitions separate then thermodynamically stable phases and the transitions



onto the solubility-temperature plane as obtained from our simulation of the 179-mer in a cavity with  $z_w = 200$ . The color code reflects the value of the specific heat and the brighter the shading, the larger the value of  $C_V$ . Black and white lines emphasize the ridges of the profile. Since we consider the specific heat as appropriate to identify pseudo-phases, these ridges mark the pseudo-phase boundaries. As expected, the pseudo-phase diagram is divided into two main parts, the phases of adsorption and desorption. The two desorbed pseudo-phases DC (desorbed-compact conformations) and DE (desorbed-expanded structures) are separated by the collapse transition line which corresponds to the  $\Theta$  transition of the infinite-length polymer which is allowed to extend into the three spatial dimensions [33]. The region of the adsorbed pseudo-phases is much more complex, and little is known about its details, since it is relevant at lower temperatures, where conventional Monte Carlo methods with pivot-like updates usually tend to fail. The presence of general phases of adsorbed-expanded (AE) [34] and adsorbed-compact (AC1, AC2) conformations was postulated in adsorption studies of grafted polymers and the existence of an additional phase of surface-attached globules (AG) [34] was assumed [16, 17, 19]. In a recent study [19], it was argued that the layering transition between AC1 and AC2 is a thermodynamic phase transition. Although the polymer in our study is still relatively small, we can clearly identify pseudo-phases in Fig. 2 which can be assigned these labels, too. Those regions are separated by the black lines indicating the transitions between them. We expect that these are transitions in the thermodynamic meaning; only the precise location of the transition lines will still change with increasing length of the polymer. Thus, this picture confirms the previously assumed phases and it provides evidence that the AG phase is indeed there. Furthermore, we have also highlighted by white lines transitions between pseudo-phases which will probably not survive in the thermodynamic limit. This concerns, e.g., the higher-order layering transitions among the compact pseudo-phases AC2a<sub>1,2</sub>-d. In the following sections we will analyse the properties of the pseudo-phases in more detail.

## B. Contact-number fluctuations

The contact numbers  $n_s$  and  $n_m$  can be considered as system parameters appropriately describing the state of the system and are therefore useful to identify the pseudo-phases. Peaks and dips in the external-parameter dependence of self-correlations  $\langle n_s^2 \rangle_c$ ,  $\langle n_m^2 \rangle_c$  and cross-correlations  $\langle n_s n_m \rangle_c$  indicate activity in the contact-number fluctuations and, analysing the

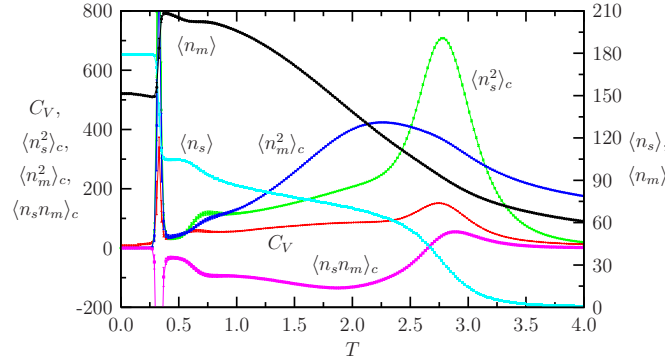


FIG. 3: (Color online) Expectation values, self- and cross-correlations of the contact numbers  $n_s$  and  $n_m$  as functions of the temperature  $T$  in comparison with the specific heat for a 179-mer in solvent with  $s = 1$ .

expectation values  $\langle n_s \rangle$  and  $\langle n_m \rangle$  in these active regions of the external parameters  $T$  and  $s$ , allow for an interpretation of the respective conformational transitions between the pseudo-phases.

In Fig. 3, we have plotted for the 179-mer these quantities and, for comparison, the specific heat as functions of the temperature  $T$  at a fixed solvent parameter  $s = 1$ . This example is quite illustrative as the system experiences several conformational transitions when increasing the temperature starting from  $T = 0$  (see Fig. 2). At temperatures very close to  $T = 0$  (pseudo-phase AC1) all 179 monomers have contact to the substrate and 153 monomer-monomer contacts are formed. This is the most compact contact set being possible for *topologically two-dimensional*, film-like conformations. It should be noted, however, that approximately  $2 \times 10^{18}$  conformations (self-avoiding walks) belong to this contact set. [35] This high degeneracy is an artefact of the minimalistic lattice polymer model used. It is remarkable that the conformations with the highest number of total contacts  $n = n_s + n_m$  are film-like compact ( $n = 332$ ). All other conformations we found possess less contacts, even the most compact contact set that dominates the five-layer pseudo-phase AC2a<sub>1</sub> ( $n_s = 36$ ,  $n_m = 263$ , i.e.,  $n = 299$ ). The reason is that for low temperatures, those macrostates are formed which are energetically favored. Entropy is not yet relevant – for the  $s = 1$  example  $\langle n_s \rangle$  drops to 149 only up to  $T \approx 0.3$ . Increasing the temperature further, the situation dramatically changes, as can be seen in Fig. 3. In a highly cooperative process, the average number of intrinsic contacts  $\langle n_m \rangle$  significantly increases (to  $\approx 208$ ) at the expense of surface contacts ( $\langle n_s \rangle$  drops to approximately 104). Consequently, the strong

fluctuations  $\langle n_{s,m}^2 \rangle_c$  signalize a conformational transition, and the anticorrelation indicated by  $\langle n_s n_m \rangle_c$  confirms that surface contacts turn into intrinsic contacts, which indirectly leads to the conclusion that the film-like structure is given up in favor of layered, spatially three-dimensional conformations. The system has entered subphase AGe which is the part of the phase AG, where two-layer conformations dominate. The subphase transition near  $T \approx 0.7$  from the two-layer (AGe) to the bulky regime of AG is due to the ongoing, rather unstructured expansion of the polymer into the  $z$  direction by forming so-called surface-attached globules [17]. This is accompanied by a further reduction of surface contacts, while the number of intrinsic contacts changes weakly. Approaching  $T \approx 2.0$ , the situation is just vice versa. Intrinsic contacts dissolve and the system experiences a conformational phase transition from globular conformations in AG to random strands in AE. Crossing this transition line, the system enters the good-solvent regime. Eventually, close to  $T \approx 2.8$ , the polymer unbinds off the substrate. A clear signal is observed in the fluctuations of  $n_s$ , i.e., the number of average surface contacts rapidly decreases. The expanded polymer is “free” and the influence of *both* walls is effectively steric. This phase (AE) is closely related to the typical random-coil phase of entirely free and dissolved polymers in good solvent.

This example shows that a study of the contact number fluctuations is indeed sufficient to qualitatively identify and describe the conformational transitions between the pseudo-phases of the hybrid system. For this reason,  $n_s$  and  $n_m$  are adequate system parameters playing a similar role as order parameters in thermodynamic phase transitions.

### C. Anisotropic behavior of gyration tensor components

One of the most interesting structural quantities in studies of polymer phase transitions is the gyration tensor (5). For our hybrid system we expect that the respective components parallel (6) and perpendicular (7) to the substrate will behave differently when the polymer passes pseudo-transition lines. In order to prove this anisotropy explicitly, we have plotted in Fig. 4 the expectation values,  $\langle R_{\parallel,\perp} \rangle$ , and the fluctuations of these two components,  $d\langle R_{\parallel,\perp} \rangle/dT$ , again for the polymer in solvent with  $s = 1$ . For interpreting the peaks of the fluctuations, we have also included once more the specific heat curve for comparison. The immediate observation is that the temperatures, where one or both gyration tensor components exhibit peaks, almost perfectly coincide with those of the specific heat. This is

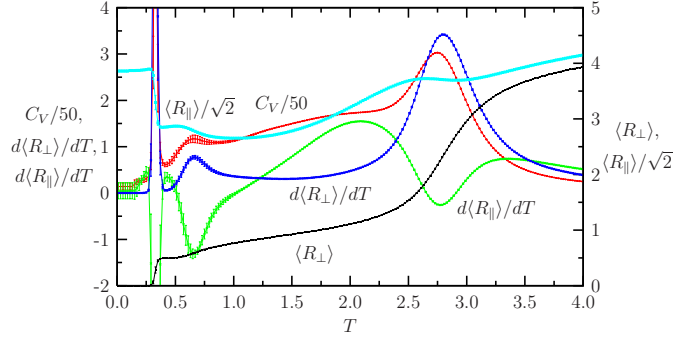


FIG. 4: (Color online) Anisotropic behavior of gyration tensor components parallel and perpendicular to the substrate and their fluctuations as functions of the temperature  $T$  for a 179-mer at  $s = 1$ . For comparison, we have also plotted the associated specific-heat curve.

a strong confirmation for the phase diagram in Fig. 2 which is based on the specific heat. Obviously, even for the rather short polymer with 179 monomers, we encounter the onset of fluctuation collapse near the (pseudo-)phase transitions. This is very promising for future quantitative finite-size scaling analyses.

At very low temperatures, i.e., in pseudo-phase AC1, we have argued in the previous section that the polymer-conformation is the most compact single-layer film. This is confirmed by the behavior of  $\langle R_{\parallel} \rangle$  and  $\langle R_{\perp} \rangle$ , the latter being zero in this phase. A simple argument that the structure is indeed maximally compact is as follows. It is well known that the most compact shape in the two-dimensional continuous space is the circle. For  $n$  monomers residing in it,  $n \approx \pi r^2$ , where  $r$  is the (dimensionless) radius of this circle. The usual squared gyration radius is

$$R_{\text{gyr}}^{\text{circ}^2} (\approx R_{\parallel}^2) = \frac{1}{\pi r^2} \int_{r' \leq r} d^2 r' r'^2 = \frac{1}{2} r^2 \quad (9)$$

and therefore  $R_{\text{gyr}}^{\text{circ}} \approx \sqrt{n/2\pi} \approx 5.34$  for  $n = N = 179$ . Indeed, this is close to the value  $R_{\parallel} \approx 5.46$  of the ground-state conformation we identified in phase AC1. Note that the most compact shape in the simple lattice polymer model we used in our study is a square and not a discretized circle. [36]

Near  $T \approx 0.3$ , the strong layering transition from AC1 to AGe is accompanied by an immediate decrease of  $\langle R_{\parallel} \rangle$ , while  $\langle R_{\perp} \rangle$  rapidly increases from zero to about 0.5 which is exactly the gyration radius (perpendicular to the layers) of a two-layer system, where both layers cover approximately the same area. Note that the single layers are still compact,

but not maximally. Applying the same approximation as in Eq. (9), the planar gyration radius for each of the two layers is now (with  $n \approx N/2$ )  $R_{\text{gyr}}^{\text{circ}} \approx 3.77$ , while we measured in this phase (AGe)  $R_{\parallel} \approx 4.05$ . This separates the subphase AGe from the other two-layer pseudo-phase AC2d in Fig. 2, where the dominating conformation has perfect two-layer (lattice) structure with  $R_{\parallel} \approx 3.85$  (this is the same 2% difference between continuous and lattice calculation for perfect shapes as above). We will discuss the conformational peculiarities in the following in more detail. The subphase transition from AGe to AG near  $T \approx 0.7$  is accompanied by a further decrease of  $\langle R_{\parallel} \rangle$  whereas  $\langle R_{\perp} \rangle$  increases, i.e., the height of the surface-adsorbed globule increases at the expense of the width. This tendency is stopped when approaching the transition ( $T \approx 2.0$ ) from the globular regime AG to the phase of expanded, but still adsorbed conformations. While  $\langle R_{\perp} \rangle$  remains widely constant (the fluctuation does not signalize any transition), the polymer strongly extends in the directions parallel to the substrate, as indicated by the peak of  $d\langle R_{\parallel} \rangle/dT$ . After unbinding from the substrate, parallel and perpendicular gyration radii behave widely isotropically ( $\langle R_{\perp} \rangle^2 \approx \langle R_{\parallel} \rangle^2/2 \approx \langle R_{\text{gyr}} \rangle^2/3$ ) as the influence of the isotropy-disturbing walls is weak in this regime.

#### IV. THE WHOLE PICTURE: THE FREE-ENERGY LANDSCAPE

It was shown in Sect. IIIB that the contact numbers  $n_s$  and  $n_m$  are unique system parameters for the pseudo-phase identification of the hybrid system. We define the restricted partition sum for a macrostate with  $n_s$  surface contacts and  $n_m$  monomer-monomer contacts by

$$\begin{aligned} Z_{T,s}(n_s, n_m) &= \sum_{n'_s, n'_m} \delta_{n'_s n_s} \delta_{n'_m n_m} g_{n'_s n'_m} e^{-E_s(n'_s, n'_m)/k_B T} \\ &= g_{n_s n_m} e^{-E_s(n_s, n_m)/k_B T}, \end{aligned} \quad (10)$$

such that  $Z = \sum_{n_s, n_m} Z_{T,s}(n_s, n_m)$ . Assuming as usual that the dominating macrostate is given by the minimum of the free energy as a function of appropriate system parameters, it is useful to define the specific contact free energy as a function of the contact numbers  $n_s$  and  $n_m$ ,

$$\begin{aligned} F_{T,s}(n_s, n_m) &= -k_B T \ln g_{n_s n_m} e^{-E_s(n_s, n_m)/k_B T} \\ &= E_s(n_s, n_m) - TS(n_s, n_m), \end{aligned} \quad (11)$$

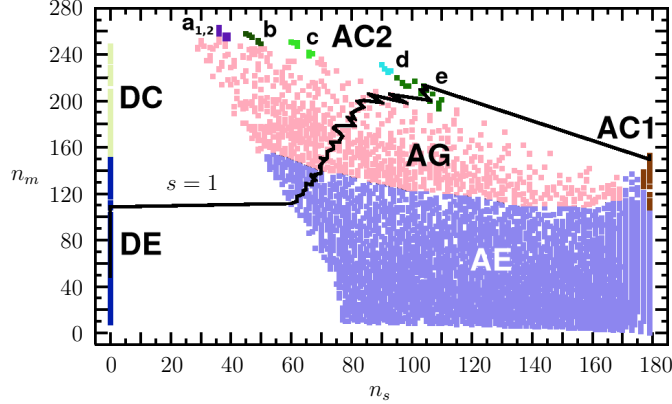
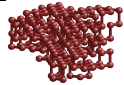
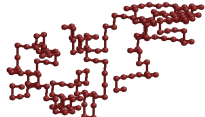
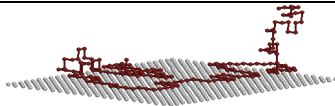
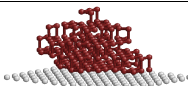
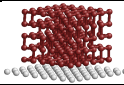
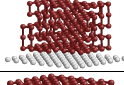
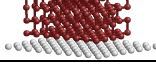
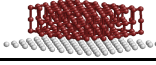
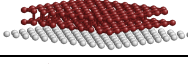


FIG. 5: (Color online) Map of all minima of the contact free energy  $F_{T,s}(n_s, n_m)$  in the parameter intervals  $T \in [0, 10]$  and  $s \in [-2, 10]$  for the 179-mer. The solid line connects the free-energy minima taken by the polymer in solvent with  $s = 1$  by increasing the temperature from  $T = 0$  to  $T = 5$  and thus symbolizes its “path” through the free-energy landscape. The solid line is only a guide to the eyes.

identifying  $k_B \ln g_{n_s n_m} \equiv S(n_s, n_m)$  as a “micro-contact” entropy. For given external parameters  $T$  and  $s$ , this relation can be used to determine the minimum of the contact free energy and therefore allows the identification of the dominant macrostate with respect to the contact numbers. In turn, this quantity allows for an alternative representation of the pseudo-phase diagram, complementary to the one shown in Fig. 2 in that it is related to the contact numbers  $n_s$  and  $n_m$ . This is done by determining for (in principle) all values of the external parameters  $T$  and  $s$  the minima of the contact free energy (11). Then the pair of values  $n_s$  and  $n_m$  of the minimum contact free-energy state are marked in an  $n_s$ - $n_m$  phase diagram. This is shown in Fig. 5, where all free-energy minima of the 179-mer for the parameter set  $T \in [0, 10]$  and  $s \in [-2, 10]$  are included and, based on the arguments of the previous section, differently shaded according to the pseudo-phase they belong to. The nice thing of this representation is that it allows the differentiation of continuous and discontinuous pseudo-phase transitions.

The first important observation is that the diagram is divided into two separate regions, the pseudo-phases of desorbed conformations (DC and DE) and the remaining different phases of adsorption. The “space” in between is blank, i.e., none of these (possible) conformations was found to be a free-energy minimum conformation. This shows that transitions between the adsorbed and desorbed pseudo-phases are always first-order-like. It should be

TABLE I: Representative minimum free-energy examples of conformations in the different pseudo-phases of a 179-mer in a cavity. The substrate is shaded in lightgray.

pseudo-phase	example	$n_s$	$n_m$
DC		0	219
DE		0	50
AE		135	33
AG		49	227
AC2a <sub>1</sub>		36	263
AC2a <sub>2</sub>		39	256
AC2b		46	257
AC2c		60	251
AC2d		90	231
AGe		103	207
AC1		179	153

noted, that the regime of contact pairs  $(n_s, n_m)$  lying *above* the shown compact phases is forbidden, i.e., conformations with such contact numbers do not exist on the sc lattice.

The second remarkable result is that the pseudo-phases DC, DE, AE, and AG are “bulky”, while all AC subphases are highly localized in the plot of the free-energy minima. Comparing with Fig. 2, the conclusion is that conformations in the AC phases are energetically favored (more explicitly, for  $s/T > 0.8$  in AC1 and  $s/T > 2.2$  in the AC2 subphases), while the behavior in the other pseudo-phases is entropy-dominated: The number of conformations with similar contact numbers in the globular or expanded regime is higher than the rather exceptional conformations in the compact phases, i.e., for sufficiently small  $s/T$  ratios the entropic effect overcompensates the energetic contribution to the free energy.

The subphases AC2a<sub>1,2-d</sub> are strongly localized, thorn-like “peninsulas” standing out from

the AG regime. The discrete number and their separation leads to the conclusion that they have related structures. Indeed, as can be seen in Table I, where we have listed representative conformations for all pseudo-phases, the few conformations dominating these subphases exhibit compact layered structures. The most compact three-dimensional conformation with 263 monomer-monomer contacts and 36 surface contacts is favored in subphase AC2a<sub>1</sub> and possesses five layers. Starting from this subphase and increasing the temperature, two things may happen. A rather small change is accompanied with the transition to AC2a<sub>2</sub>, where the number of intrinsic contacts is reduced but the global five-layer structure remains. On the other hand, passing the transition line towards AC2b, the monomers prefer to arrange in compact four-layer conformations. Advancing towards AC2d, the typical conformations reduce layer by layer in order to increase the number of surface contacts. In AC2d there are still two layers lying almost perfectly on top of each other. This is similar in subphase AGe, where also two-layer but less compact conformations dominate. In pseudo-phase AC1 only the film-like surface layer remains. The reason for the differentiation of the phases AC1 and AC2 of layered conformations is that the transition from single- to double-layer conformations is expected to be a real phase transition, while the transitions between the higher-layer AC2 subphases are assumed to disappear in the thermodynamic limit. [19]

As can be seen in Fig. 2, a transition between AC1 and the phase of adsorbed, expanded conformations, AE, is possible. Since these two phases are connected in Fig. 5, we expect that the transition in between is second-order-like. Indeed, this transition is strongly related with the *two-dimensional*  $\Theta$  transition since, close to the transition line, all monomers form a planar (surface-)layer. Similarly, there is also a second-order-like transition line  $s_0(T)$  between AG and AE which separates the regions of poor (AG:  $s > s_0$ ) and good (AE:  $s < s_0$ ) solvent. Also, the transition between the desorbed compact (DC) and expanded (DE) conformations is second-order-like: This transition is strongly related with the well-known  $\Theta$  transition in three dimensions. [31] Eventually, the transitions from the layer-phases AC2a<sub>2</sub>, AC2b, AC2c, and AGe to the globular pseudo-phase AG as well as transitions between pseudo-phases dominated by the same layer type (i.e., between the two-layer subphases AC2d and AGe, and between the five-layer subphases AC2a<sub>1</sub> and AC2a<sub>2</sub>) are expected to be continuous.

On the other hand, the transitions among the energetically caused compact low-temperature pseudo-phases are rather first-order-like, due to their noticeable localization in

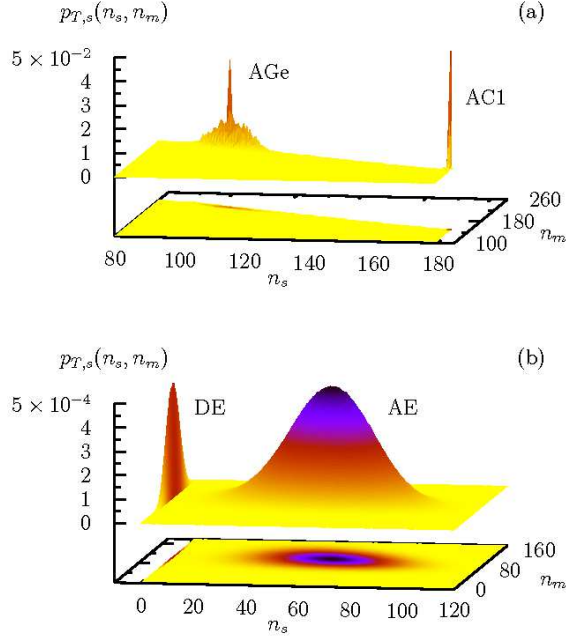


FIG. 6: (Color online) Probability distributions  $p_{T,s}(n_s, n_m)$  for the 179-mer in solvent with  $s = 1$  (a) near the layering transition from AC1 to AGe at  $T \approx 0.34$  and (b) near the adsorption-desorption transition from AE1 to DE at  $T \approx 2.44$ . Both transitions are expected to be real phase transitions in the thermodynamic limit and look first-order-like.

the map of free-energy minima (Fig. 5). The possible transitions (see Fig. 2) are AC2a<sub>1,2</sub>–AC2b, AC2b–AC2c, and AC2c–AC2d, respectively. Even more interesting, however, are the transitions from the single-layer pseudo-phase AC1 to the double-layer subphases AC2d and AGe. In the previous sections we already discussed this transition for the special choice  $s = 1$ , where near  $T \approx 0.3$  the fluctuations of the contact numbers and the components of the gyration tensor exhibit a strong activity. We have included into Fig. 5 the “path” of macrostates the system passes by increasing the temperature from  $T = 0$  to  $T = 5$ . At  $T = 0$  the system is in a film-like, single-layer state. Near  $T \approx 0.3$  it indeed suddenly rearranges into two layers and enters subphase AGe in a single step. In Fig. 6(a) we have plotted the probability distribution  $p_{T,s}(n_s, n_m)$  for  $s = 1$  and  $T = 0.34$  and it can clearly be seen that two distinguished macrostates coexist. [37, 38] Increasing the temperature further, the system undergoes the continuous transitions from AGe via AG until it unfolds when entering pseudo-phase AE. The system is still in contact with the substrate. Close to a tem-

perature  $T \approx 2.4$ , however, the unbinding of the polymer off the substrate happens (from AE to DE). Comparing Figs. 5 and 6(b), where the probability distribution at  $T = 2.44$  is shown, we see also a clear indication for a discontinuous transition. Note that we consider here the transition state, where the two minima of the free energy coincide [39] (see also the black dashed line in Fig. 2) and not the point, where the width of the distribution, i.e., the specific heat, is maximal. Since the system is finite, the transition temperature ( $T \approx 2.8$ ), as signalled by the fluctuations studied in the previous sections, deviates slightly from the transition-state temperature reported here.

## V. SUMMARY

In this paper, we have studied in detail the solubility-temperature (pseudo-)phase diagram of a polymer in a cavity with an attractive substrate. We identified the thermodynamic phases of adsorbed compact and expanded (AC, AE) and desorbed (DC [33], DE) conformations as well as the previously not yet clearly confirmed phase of adsorbed globules (AG). Although the polymer in our study possessed only  $N = 179$  monomers, these (pseudo-)phases are expected to be stable also in the thermodynamic limit  $N \rightarrow \infty$ . Other noticeable phase transitions in the compact-globular adsorbed regime (AC1-AC2d, AC1-AGe) are the energetic layering transitions from film-like surface-layer to double-layer conformations which are also believed to survive the thermodynamic limit. [19] In addition, further subphases of higher-order layers were found in low-temperature regions and bad solvent (AC2a<sub>1,2</sub>, AC2b, and AC2c). The most compact three-dimensional conformation found is cube-like and forms five layers (in subphase AC2a<sub>1</sub>).

The (pseudo-)phase diagram is based on the specific-heat profile as a function of temperature and reciprocal solubility. Although this profile allows for the identification of phases and their boundaries it does tell little about the conformational transitions between the phases. For this purpose we considered expectation values and fluctuations for the numbers of monomer-surface contacts,  $n_s$ , and intrinsic monomer-monomer contacts,  $n_m$ , separately. These contact numbers turned out to be sufficient to describe the macrostate of the system and therefore are useful to describe the conformations dominating the different phases. This view was completed by an exemplified study of the anisotropic behavior of the gyration tensor components of the polymer parallel and perpendicular to the substrate.

Another central aspect was the classification of the conformational transitions between the (pseudo-)phases. Based on the contact numbers  $n_s$  and  $n_m$ , we defined an appropriate free energy and studied the distribution of the minima in the  $n_s$ - $n_m$  space. From this kind of free-energy landscape, we found strong indications that the binding-unbinding transitions between the adsorbed and desorbed phases are first-order-like. This was also observed for the layering transitions. On the other hand, the transitions across the line separating good and poor solvent, i.e., between the compact (or globular) and the expanded conformations, are rather second-order-like. This is in coincidence with the known behavior of free polymers at the  $\Theta$  collapse transition in two and three dimensions.

Since the experimental equipment and the technological capabilities have nowadays reached an enormous standard of high single-molecular resolution, we expect that it should be possible to verify experimentally not only the existence of the described thermodynamic phases, but also the pseudo-phases being only relevant for finite polymers and specific to their lengths.

## VI. ACKNOWLEDGEMENTS

This work is partially supported by the DFG (German Science Foundation) grant under contract No. JA 483/24-1. Some simulations were performed on the supercomputer JUMP of the John von Neumann Institute for Computing (NIC), Forschungszentrum Jülich, under grant No. hlz11.

- 
- [1] S. Brown, *Nature Biotechnol.* **15**, 269 (1997).
  - [2] S. R. Whaley, D. S. English, E. L. Hu, P. F. Barbara, A. M. Belcher, *Nature* **405**, 665 (2000).
  - [3] K. Goede, P. Busch, and M. Grundmann, *Nano Lett.* **4**, 2115 (2004).
  - [4] R. L. Willett, K. W. Baldwin, K. W. West, and L. N. Pfeiffer, *Proc. Natl. Acad. Sci. (USA)* **102**, 7817 (2005).
  - [5] J. J. Gray, *Curr. Opin. Struct. Biol.* **14**, 110 (2004).
  - [6] G. Reiter, *Phys. Rev. Lett.* **87**, 186101 (2001).

- [7] J. Forsman and C. E. Woodward, *Phys. Rev. Lett.* **94**, 118301 (2005).
- [8] E. Nakata, T. Nagase, S. Shinkai, and I. Hamachi, *J. Am. Chem. Soc.* **126**, 490 (2004).
- [9] T. Bogner, A. Degenhard, and F. Schmid, *Phys. Rev. Lett.* **93**, 268108 (2004).
- [10] E. Balog, T. Becker, M. Oettl, R. Lechner, R. Daniel, J. Finney, and J. C. Smith, *Phys. Rev. Lett.* **93**, 028103 (2004).
- [11] M. Ikeguchi, J. Ueno, M. Sato, and A. Kidera, *Phys. Rev. Lett.* **94**, 078102 (2005).
- [12] N. Gupta and A. Irbäck, *J. Chem. Phys.* **120**, 3983 (2004).
- [13] C.-H. Cheng and P.-Y. Lai, *Phys. Rev. E* **71**, 060802(R) (2005).
- [14] G. M. Foo and R. B. Pandey, *Phys. Rev. Lett.* **80**, 3767 (1998); *Phys. Rev. E* **61**, 1793 (2000).
- [15] R. Hegger and P. Grassberger, *J. Phys. A* **27**, 4069 (1994).
- [16] T. Vrbová and S. G. Whittington, *J. Phys. A* **29**, 6253 (1996); *J. Phys. A* **31**, 3989 (1998);  
T. Vrbová and K. Procházka, *J. Phys. A* **32**, 5469 (1999).
- [17] Y. Singh, D. Giri, and S. Kumar, *J. Phys. A* **34**, L67 (2001); R. Rajesh, D. Dhar, D. Giri, S. Kumar, and Y. Singh, *Phys. Rev. E* **65**, 056124 (2002).
- [18] M. S. Causo, *J. Chem. Phys.* **117**, 6789 (2002).
- [19] J. Krawczyk, T. Prellberg, A. L. Owczarek, and A. Rechnitzer, *Europhys. Lett.* **70**, 726 (2005).
- [20] J.-H. Huang and S.-J. Han, *J. Zhejiang Univ. SCI.* **5**, 699 (2004).
- [21] M. Breidenreich, R. R. Netz, and R. Lipowsky, *Europhys. Lett.* **49**, 431 (2000); *Eur. Phys. J. E* **5**, 403 (2001).
- [22] P. Benetatos and E. Frey, *Phys. Rev. E* **70**, 051806 (2004).
- [23] F. Celestini, T. Frisch, and X. Oyharcabal, *Phys. Rev. E* **70**, 012801 (2004).
- [24] J. Krawczyk, T. Prellberg, A. L. Owczarek, and A. Rechnitzer, *J. Stat. Mech.* (2004), P10004.
- [25] M. Bachmann and W. Janke, *Phys. Rev. Lett.* **95**, 058102 (2005).
- [26] M. Bachmann and W. Janke, submitted (2005).
- [27] M. Bachmann and W. Janke, *Phys. Rev. Lett.* **91**, 208105 (2003); *J. Chem. Phys.* **120**, 6779 (2004).
- [28] A related flat-histogram chain-growth method was introduced in: T. Prellberg and J. Krawczyk, *Phys. Rev. Lett.* **92**, 120602 (2004).
- [29] P. Grassberger, *Phys. Rev. E* **56**, 3682 (1997).
- [30] M. N. Rosenbluth and A. W. Rosenbluth, *J. Chem. Phys.* **23**, 356 (1955).
- [31] P. D. de Gennes, *Scaling Concepts in Polymer Physics* (Cornell University Press, Ithaca,

- 1979).
- [32] F. Rampf, W. Paul, and K. Binder, *Europhys. Lett.* **70**, 628 (2005).
- [33] In very poor solvent (i.e., very large values of  $s$ ), the DC phase may degenerate, at least for the finite-length polymers, into separate globular and crystalline subphases (see, e.g., Ref [32]), but this effect is not in the focus of the present study of adsorption properties.
- [34] In our recent study of a 100-mer in a cavity, [25] we have still denoted AE as AE1 and AG as AE2, because the differentiation between these two phases was still relatively diffuse due to the small size of the system. For the longer chain we are considering here, the identification of these phases is much clearer.
- [35] An enormous advantage of the simple-sampling algorithms based on Rosenbluth sampling [30] compared to importance-sampling methods is that they allow the approximation of the degeneracy (“density”) of states *absolutely*, i.e., free energy and entropy can explicitly be determined.
- [36] This is also true for most compact three-dimensional structures which are cube-like. Therefore, globules in the lattice model are rather cubes than spheres!
- [37] C. Borgs and W. Janke, *Phys. Rev. Lett.* **68**, 1738 (1992); W. Janke, *Phys. Rev. B* **47**, 14757 (1993).
- [38] W. Janke, *First-Order Phase Transitions*, in: *Computer Simulations of Surfaces and Interfaces*, NATO Science Series, II. Mathematics, Physics and Chemistry – Vol. **114**, Proceedings of the NATO Advanced Study Institute, Albena, Bulgaria, 9 – 20 September 2002, edited by B. Dünweg, D. P. Landau, and A. I. Milchev (Kluwer, Dordrecht, 2003), p. 111.
- [39] Strictly speaking, the proper definition of the coexistence point is the temperature, where the weights under the two peaks are equal, see, e.g., Refs. [37, 38].